Human Molecular Genetics, 2016, Vol. 25, No. 22 5017–5026

doi: 10.1093/hmg/ddw332
Advance Access Publication Date: 7 October 2016
Original Article

ORIGINAL ARTICLE

Chronic pancreatitis and lipomatosis are associated with defective function of ciliary genes in pancreatic ductal cells

Cécile Augereau[1,†], Louis Collet[1,†], Pierfrancesco Vargiu[2], Carmen Guerra[3], Sagrario Ortega[2], Frédéric P. Lemaigre[1] and Patrick Jacquemin[1,*]

[1]Université catholique de Louvain, de Duve Institute, Brussels, Belgium, [2]Transgenic Mice Core Unit and [3]Molecular Oncology, Centro Nacional de Investigaciones Oncológicas, Madrid, Spain

*To whom correspondence should be addressed at: Patrick Jacquemin, Université catholique de Louvain, de Duve Institute, Avenue Hippocrate 75 bte B1.75.03, B-1200 Brussels, Belgium. Tel: +32.2.764.75.31, Fax: +32.2.764.75.07. Email: patrick.jacquemin@uclouvain.be

Abstract

Genetic diseases associated with defects in primary cilia are classified as ciliopathies. Pancreatic lesions and ductal cysts are found in patients with ciliopathic polycystic kidney diseases suggesting a close connection between pancreatic defects and primary cilia. Here we investigate the role of two genes whose deletion is known to cause primary cilium defects, namely Hnf6 and Lkb1, in pancreatic ductal homeostasis. We find that mice with postnatal duct-specific deletion of Hnf6 or Lkb1 show duct dilations. Cells lining dilated ducts present shorter cilia with swollen tips, suggesting defective intraciliary transport. This is associated with signs of chronic pancreatitis, namely acinar-to-ductal metaplasia, acinar proliferation and apoptosis, presence of inflammatory infiltrates, fibrosis and lipomatosis. Our data reveal a tight association between ductal ciliary defects and pancreatitis with perturbed acinar homeostasis and differentiation. Such injuries can account for the increased risk to develop pancreatic cancer in Peutz-Jeghers patients who carry LKB1 loss-of-function mutations.

Introduction

Cilia are evolutionarily conserved, antenna-like organelles that protrude from the cells into the extracellular environment and transduce signals from extracellular stimuli to the recipient cells. Over the last decade accumulating evidences have shown the biological importance of the primary cilium. Disruption of cilium structure or function is responsible for an increasing number of disorders categorized as ciliopathies (1,2). These diseases have shed light on the role of cilia as sensors and signalling hubs (3–6).

Like in other organs, ciliary defects are associated with dysfunctions of the pancreas. In this organ, exocrine functions are exerted by the acinar cells, which secrete digestive enzymes, and by the ductal cells lining the ducts, which transport and modify acinar secretions to the duodenum. Within the pancreas, ductal and islet cells are ciliated whereas acinar cells are not. A link between ciliary defects and pancreatic abnormalities was initially suggested by the observation that patients with autosomal dominant polycystic kidney disease (ADPKD; OMIM entry #173900), a ciliopathy, have pancreatic cysts and develop chronic pancreatitis (7,8). Subsequently mouse models revealed that deletion of ciliary genes leads to cystic ducts, acinar-to-ductal metaplasia, acinar apoptosis, and lipomatosis (9–11).

In the studies listed above, disruption of the ciliary genes, cyst formation and ciliary defects were initiated during the

[†]Contributed equally to the present work.

Received: April 15, 2016. **Revised:** September 23, 2016. **Accepted:** September 25, 2016

foetal period. In addition, this disruption abolished gene functions in all pancreatic cell types, leaving open the question of the cell type whose defect is causing the diseases. Since cilia are found in duct cells and not acinar cells, specific ductal ablation of genes involved in ciliary function is essential to fully understand the role of cilia in the pancreas (11).

Transcription factor Hepatocyte Nuclear Factor 6 (Hnf6/Onecut1) is involved in key aspects of pancreas development (12–14), including in pancreatic duct development: constitutive inactivation of Hnf6 leads to pancreatic cyst formation characterized by the absence of primary cilia during embryogenesis (15). Likewise, the tumour suppressor Liver Kinase B1/Serine/Threonine Kinase 11 (Lkb1/Stk11) has also been involved in the development of pancreatic cysts (16). No link has currently been established between the pancreatic deletion of Lkb1, the presence of these cysts and ciliary defects. However, such a link can be hypothesised since Lkb1 is present in the primary cilium (17) and Lkb1 loss results in ciliary defects (18).

To investigate the role of Hnf6 and Lkb1 in ductal cells and their relation with primary cilia, we postnatally inactivated the two genes specifically in pancreatic ductal cells. Hnf6- and Lkb1-deficient mice displayed very similar phenotypes characterized by enlarged ducts, acinar apoptosis, acinar-to-ductal metaplasia, and lipomatosis. Importantly, both Hnf6- and Lkb1-deleted mice showed reduced length and swelling of primary cilia found in the dilated ducts, indicative of perturbed ciliary function. Our data underscore the tight association between ciliary defect and pancreatitis, suggesting that perturbed homeostasis and ciliary function of the ductal cells can cause pancreatitis with perturbed differentiation of acinar cells.

Results

Postnatal ductal deletion of Hnf6 or Lkb1 induces lipomatosis

To study the phenotypic consequences of postnatal Hnf6 loss in ductal cells, we generated mice that harbour floxed (19) and knock-out (12) Hnf6 alleles and carry a Sox9-CreER (20) transgene which allows tamoxifen-dependent and duct-specific recombination of target genes (Sox9CreER/Hnf6$^{f/-}$ mice). Nursing mothers were treated by intraperitoneal injections and gavage with tamoxifen to induce Hnf6 deletion in their offspring at postnatal days 2 to 10 by transfer of tamoxifen via milk (Fig. 1A). Hnf6 deletion was observed in about 75% of the ductal cells (Supplementary Material, Fig. S1).

Three weeks after birth, examination of Sox9CreER/Hnf6$^{f/-}$ pancreata revealed slight pancreatic abnormalities. Ductal lumens were dilated and a few infiltrating adipocytes were observed near dilated ducts (Fig. 1B). At this stage, acinar cell morphology appeared unaffected (Fig. 1B). With age, an increasing number of adipocytes were detected in the Sox9CreER/Hnf6$^{f/-}$ pancreata. This culminated in 6-month old animals with a subset of acinar lobules being entirely replaced by adipocytes (Fig. 1B).

Concomitantly, we characterized the pancreatic phenotype of mice with ductal deletion of Lkb1 (21) (Sox9CreER/Lkb1$^{f/f}$ mice). Lkb1 deletion was achieved postnatally (Fig. 1A), as described for Hnf6 inactivation. The lack of Lkb1 antibody suitable for detection of Lkb1 on PFA-fixed paraffin sections precluded to determine the efficiency with which Lkb1 was deleted in Sox9CreER/Lkb1$^{f/f}$ ducts. However the pancreatic phenotype exhibited by Sox9CreER/Lkb1$^{f/f}$ mice (see below) suggests that this deletion was efficient. Lipomatosis was detected like in Sox9CreER/Hnf6$^{f/-}$ pancreas. The phenotypic consequences of Lkb1 deletion were delayed as compared to those in the absence of Hnf6, since the effects of Lkb1 loss started to appear beyond 3 weeks of age (Fig. 1B and C). Despite extensive replacement of acinar cells by adipocytes in both mouse models, no body wasting was observed, suggesting that the remaining acini were sufficient to ensure homeostasis (data not shown).

The origin of adipocytes infiltrating the pancreas was addressed by lineage tracing. Since previous studies showed that acinar cells can transdifferentiate into adipocytes (22,23), we labelled and traced the acinar cells in Sox9CreER/Hnf6$^{f/-}$ pancreas using a doxycycline-controlled transgenic system (Supplementary Material, Fig. S2). The latter consists of an elastase promoter-driven tetracycline transactivator (tTA) expressed in acinar cells (24), which in the absence of doxycycline, binds to a TetO element located upstream of a flippase (FlpO)-coding gene. FlpO then recombines FlpO recognition target (FRT) sites flanking a stop cassette (FSF) located upstream of an YFP gene inserted in the Rosa locus (25) (Rosa FSF YFP mice), leading to YFP expression in the acinar cells (Supplementary Material, Fig. S2A). Tracing efficiency determined by YFP labelling revealed that 10% of the acinar cells were traced using this system.

In control and in Sox9CreER/Hnf6$^{f/-}$ mice, adipocytes marked by Fabp4 were found at the periphery of the pancreas or in the fat pads surrounding the ovary but none of these cells were YFP-positive (data not shown). In contrast, a few adipocytes were positive for YFP in the fatty infiltrate between or in the pancreatic lobules of Sox9CreER/Hnf6$^{f/-}$ mice (Supplementary Material, Fig. S2B). Taking into account that 10% of the acinar cells were YFP-labelled, quantification indicated that about 2% of these adipocytes derived from acinar cells in these mice. Expression of β-catenin and its target c-Myc was reduced in Sox9CreER/Hnf6$^{f/-}$ acinar cells, suggesting that defective expression of these genes contributes to acinar-to-adipocyte transdifferentiation, as observed by others in Myc-deficient acinar cells (22) (Supplementary Material, Fig. S2C). Of note, no ductal cell was detected positive for YFP using this acinar lineage tracing (data not shown). Finally, genetic lineage tracing of the ductal cells in Sox9CreER/Hnf6$^{f/-}$/Rosa LSL YFP (26) pancreas did not provide evidence for duct-to-adipocyte transdifferentiation (Supplementary Material, Fig. S2D).

Together our results indicate that ductal deletion of Hnf6 and Lkb1 induces similar phenotypes, albeit with different timing of events. Extensive lipomatosis develops, resulting for a minor part from acinar-to-adipocyte transdifferentiation.

Fibrosis and inflammation are detected in Sox9CreER/Hnf6$^{f/-}$ and Sox9CreER/Lkb1$^{f/f}$ pancreata

Masson's trichrome staining showed periductal fibrosis in mice with ductal deletion of Hnf6 and Lkb1 (Fig. 2A). Fibrotic regions were positively stained for the intermediate filament protein vimentin, a marker frequently up-regulated in pancreatitis (Fig. 2B). In control pancreata, vimentin expression was only observed around large pancreatic vessels and ducts (Fig. 2B).

As fibrosis and inflammation are often associated during pancreatitis, we also looked for the presence of inflammatory infiltrates and detected the presence of macrophages throughout pancreata of Sox9CreER/Hnf6$^{f/-}$ and Sox9CreER/Lkb1$^{f/f}$ mice (Fig. 2C). Macrophages were absent from control pancreata (Fig. 2C).

We concluded that inactivation of Hnf6 and Lkb1 leads to lipomatosis associated with chronic pancreatitis.

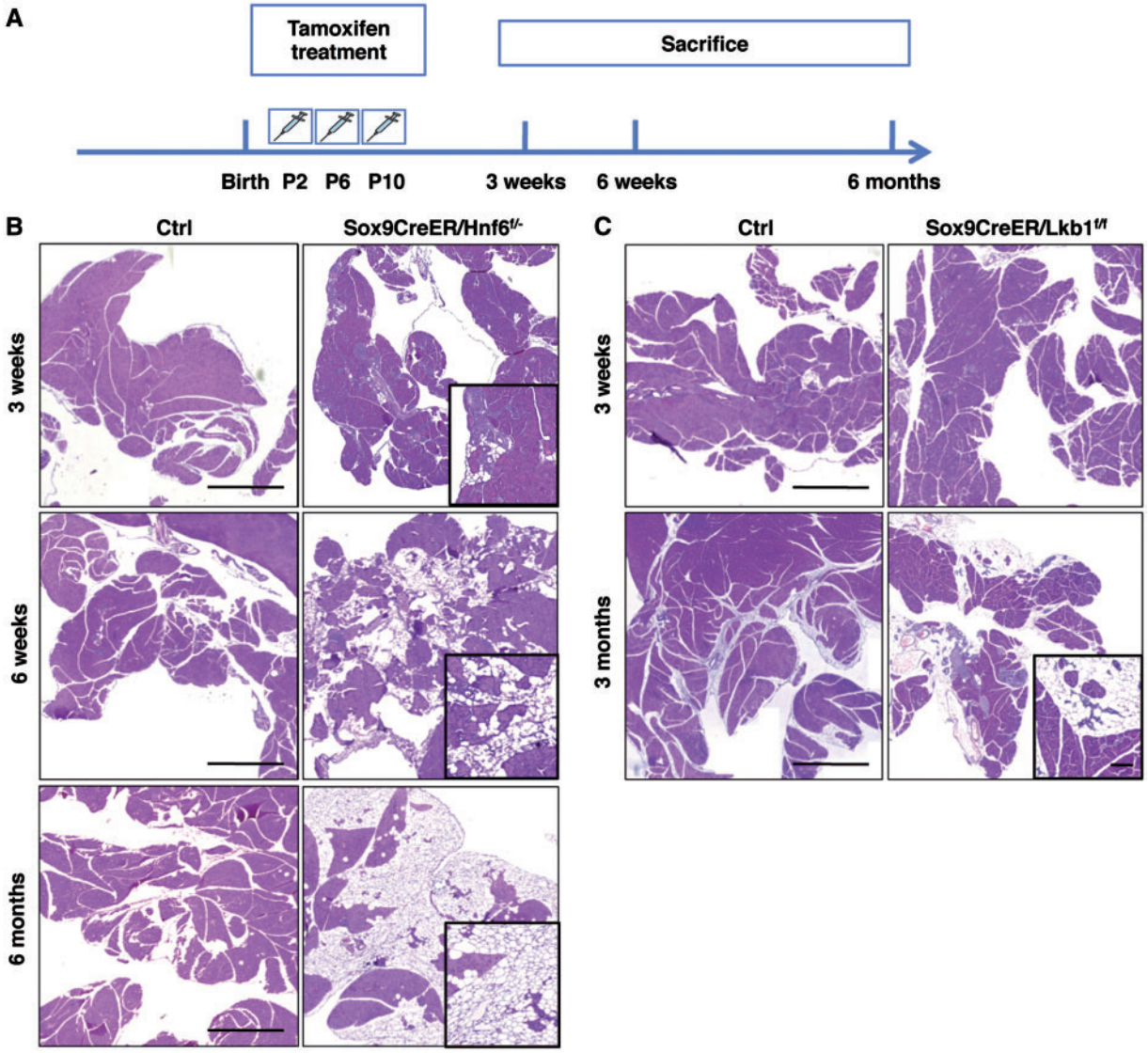

Figure 1. Histological analysis shows similar fatty infiltration in Sox9CreER/Hnf6$^{f/-}$ and Sox9CreER/Lkb1$^{f/f}$. (**A**) Schedule of Hnf6 and Lkb1 deletion. Nursing mothers were injected with tamoxifen by intraperitoneal injections and gavage at postnatal days (P) 2, 6 and 10. (**B**) Hematoxylin and eosin (H&E) staining of pancreatic tissues from control (Ctrl) and mutant mice. Three-week old Sox9CreER/Hnf6$^{f/-}$ mice show only few adipocytes with dilated ducts. At 6 weeks and 6 months, a large part of the acinar tissue is replaced by adipocytes. (**C**) Three-week old Sox9CreER/Lkb1$^{f/f}$ mice show no phenotype, while at 3 months of age, dilated ducts and adipocytes are found in the pancreatic tissue. Scale Bar= 1 mm.

Pancreatic ducts are dilated in Sox9CreER/Hnf6$^{f/-}$ and Sox9CreER/Lkb1$^{f/f}$ pancreata

Dilated pancreatic ducts were frequently observed in the fibrotic parts of Sox9CreER/Hnf6$^{f/-}$ and Sox9CreER/Lkb1$^{f/f}$ pancreata (Fig. 3A and B). Sox9 labelling and quantification of the duct area revealed that the average duct surface exhibited an 8- and 5-fold increase in Sox9CreER/Hnf6$^{f/-}$ and Sox9CreER/Lkb1$^{f/f}$ ducts, respectively, as compared to controls (Fig. 3A). No significant increase in ductal cell proliferation was observed in 3- and 6-week old pancreata in the absence of Hnf6 or in 3-week old pancreata in the absence of Lkb1 (data not shown and Fig. 3B). In contrast, hyperplastic areas of Sox9CreER/Lkb1$^{f/f}$ pancreata, showed increased ductal proliferation (Fig. 3B). This suggests that in these animals, increased ductal proliferation causes ductal dilatation.

Ductal deletion of Hnf6 or Lkb1 causes acinar-to-ductal metaplasia, proliferation, and apoptosis

Pancreatic inflammation and fibrosis are often associated with acinar-to-ductal metaplasia (ADM), a process characterized by a down-regulation of acinar genes and up-regulation of ductal genes in the metaplastic acinar cells (27). Immunofluorescent labelling for the acinar markers Mist1, Ptf1a and amylase showed decreased or lack of expression in a subset of acinar cells of the Sox9CreER/Hnf6$^{f/-}$ and Sox9CreER/Lkb1$^{f/f}$ pancreata (Fig. 4A and B).

Consistent with ADM, the transcription factors Hnf6 and Sox9 showed ectopic expression in metaplastic acinar cells, and were detected exclusively in ductal cells in control mice (Fig. 4C and D). Likewise, we also detected induction of ErbB2, a member

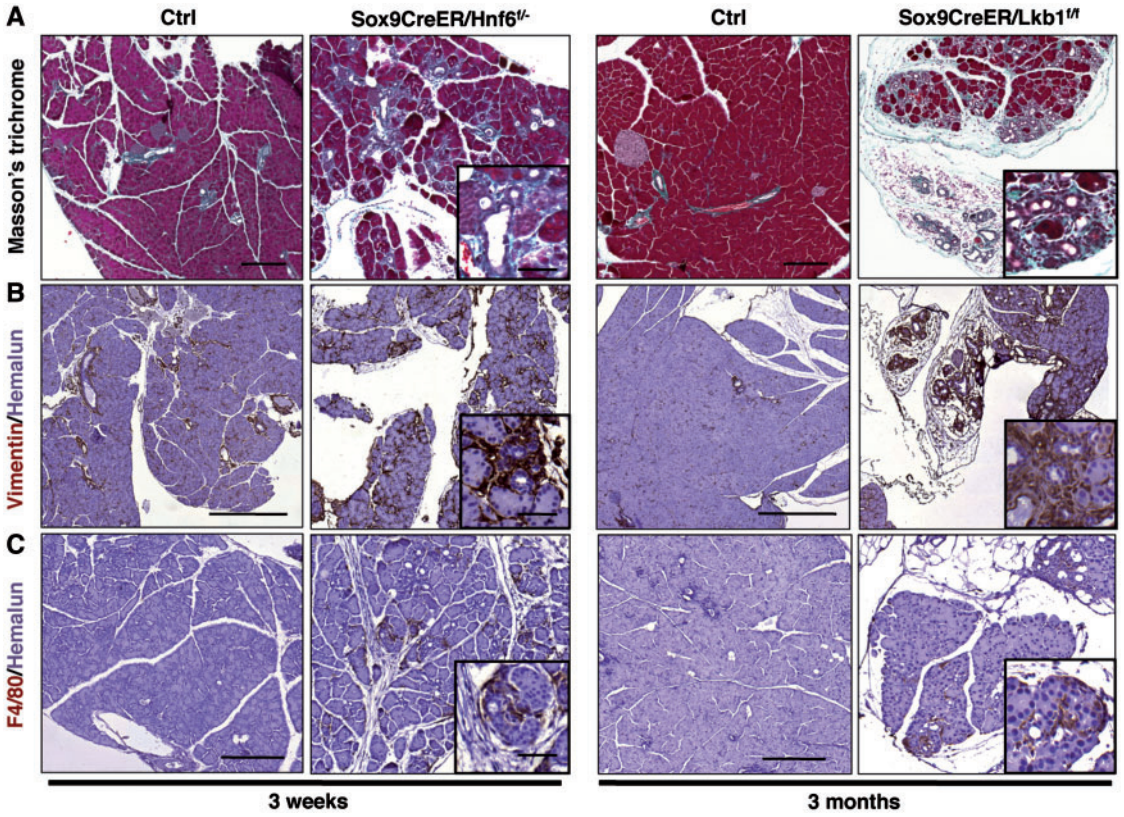

Figure 2. Phenotypic analysis of Sox9CreER/Hnf6$^{f/-}$ and Sox9CreER/Lkb1$^{f/f}$ pancreata. (**A**) Masson's trichrome staining (blue-green) reveals significant increase in collagen deposition in periductal regions in Sox9CreER/Hnf6$^{f/-}$ and Sox9CreER/Lkb1$^{f/f}$ pancreas. Scale bar= 200 μm. (**B**) Staining for the intermediate filament vimentin confirms the presence of fibrosis in Sox9CreER/Hnf6$^{f/-}$ and Sox9CreER/Lkb1$^{f/f}$ pancreata. Scale bar= 500 μm. (**C**) F4/80 staining shows the presence of macrophages in Sox9CreER/Hnf6$^{f/-}$ and Sox9CreER/Lkb1$^{f/f}$ mice. Scale bar= 200 μm, inset= 50 μm.

of the Epidermal Growth Factor Receptor (EGFR) pathway known to be induced in metaplastic cells (28,29) (Fig. 5E).

Proliferation of acinar cells in mutant pancreas was assessed by immunolabeling of Ki67. In Sox9CreER/Hnf6$^{f/-}$ pancreata, significantly increased proliferation was detected starting at 6-weeks of age (Fig. 5A). Average proliferation was increased 3-fold in Sox9CreER/Lkb1$^{f/f}$ pancreata at 3 months. However, due to high variability between metaplastic areas in Lkb1-deficient pancreata, the latter results were not statistically significant (Fig. 5C). Metaplastic areas in mutant Sox9CreER/Hnf6$^{f/-}$ and Sox9CreER/Lkb1$^{f/f}$ pancreata also showed increased numbers of apoptotic acinar cells, as detected by TUNEL staining (Fig. 5B and D).

Together, these data suggest that ductal deletion of Hnf6 or Lkb1 induces pancreatitis associated with acinar-to-ductal metaplasia, apoptosis and proliferation of acinar cells.

Defective cilia are found in Hnf6- and Lkb1-deficient ductal cells

Similarities between mice lacking Hnf6 or Lkb1 in their pancreatic ductal cells suggest that both phenotypes depend on overlapping mechanisms. Since deletion of these genes in embryonic cells results in loss of primary cilia (15,18), we analysed cilia in pancreatic ducts cells of the mutant mice. We used antibodies against acetylated tubulin, a component of the cilium axoneme, and against Arl13b, a small GTPase that localizes to cilia and regulates ciliary length and signalling (30). Cilia were present in both control and mutant mice but were reduced in length by 2.5-fold in Sox9CreER/Hnf6$^{f/-}$ and by 1.6-fold in Sox9CreER/Lkb1$^{f/f}$ ductal cells (Fig. 6A and C). Swelling of the ciliary tip was also detected (Fig. 6A and B), and this was confirmed by Z-stacking analysis (Supplementary Material, Fig. S3).

Previous reports have shown that ciliary defects, duct dilatation and apical cell polarity defects are sometimes associated (15,31). However, we found no evidence for abnormal apical polarity of the mutant ductal cells since ezrin and Mucin1A were normally located at the apical pole of the ductal cells (Supplementary Material, Fig. S4A and B). Therefore, the absence of Hnf6 or Lkb1 affects specifically the primary cilium and is not the result of global apico-basal perturbation.

Taken together, these data indicate that Hnf6 or Lkb1 deletion in pancreatic ductal cells results in ciliary defects.

Discussion

Over the last years a growing number of ciliopathies have been discovered. However, little is known about the role of primary cilia in the pancreas. Development of ductal pancreatic cysts and pancreatitis in ciliopathies like polycystic kidney diseases suggested a role of ciliary dysfunction in pancreatic disease. Pancreatic deletion of the genes coding for Kinesin Family Member 3a (Kif3a) and Intraflagellar Transport 88 (Ift88), which are required for cilium formation and maintenance, further supported this hypothesis (9–11). However these studies were

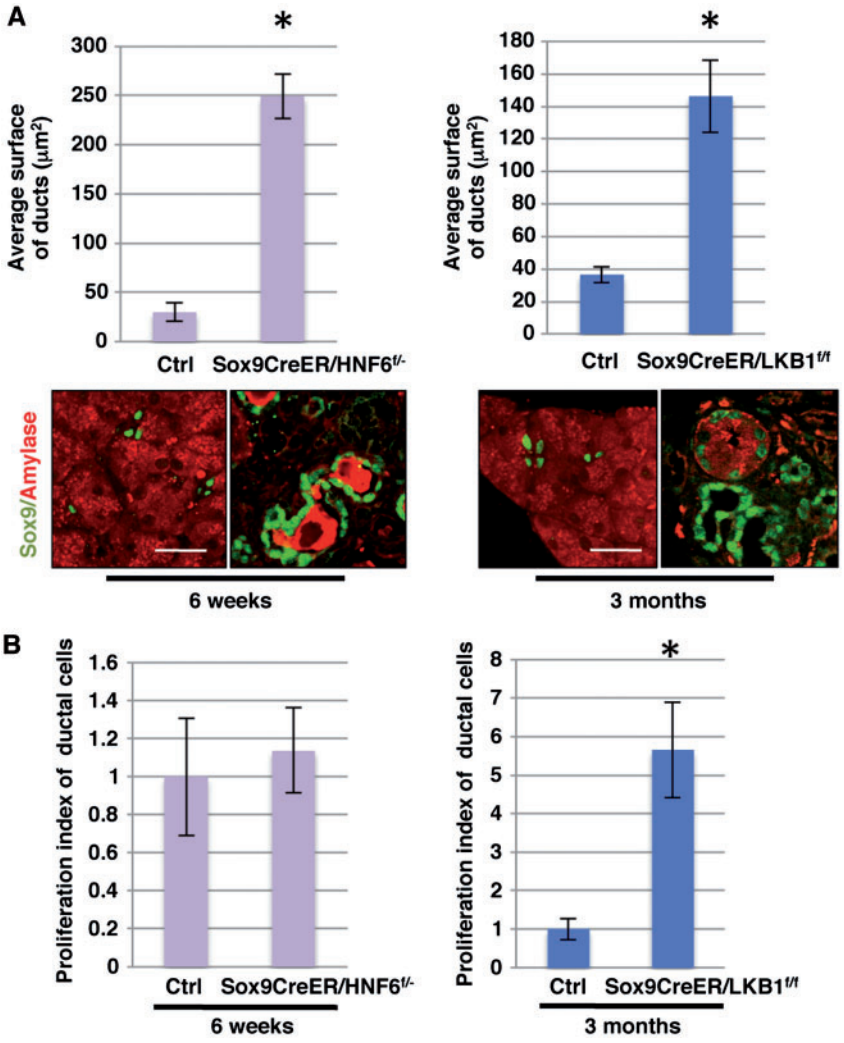

Figure 3. Pancreatic ducts are dilated in Sox9CreER/Hnf6$^{f/-}$ and Sox9CreER/Lkb1$^{f/f}$ pancreata. (**A**) Amylase and Sox9 labelling shows that ductal inactivation of Hnf6 significantly increases the surface of the pancreatic ducts by 8.3-fold (29.9 ± 9.4 vs 249.2 ± 22.7, *$P < 0.05$. Control, $n = 3$, Hnf6-deficient pancreas, $n = 3$). An identical phenotype is observed in Lkb1-deficient ducts with an increase of 4.0-fold (36.4 ± 4.9 vs 146.4 ± 22.3, *$P < 0.05$. Control, $n = 3$, Lkb1-deficient pancreas, $n = 3$). Scale bar= 20 µm (**B**) Proliferation index of ductal cells, calculated as the percentage of Sox9- Hnf1β-positive cells that are Ki67-positive cells, was determined in control (Ctrl), Sox9CreER/Hnf6$^{f/-}$ and Sox9CreER/Lkb1$^{f/f}$ pancreata. No significant difference is found between control and Hnf6-deficient pancreata at 6 weeks after birth (control, $n = 4$; Hnf6-deficient pancreas, $n = 5$). Three months after birth, Lkb1-deficient ductal cells show a 5.6-fold increased proliferation (1.0 ± 0.3 vs 5.8 ± 1.3, *$P < 0.05$), as compared to control mice (control, $n = 3$, Lkb1-deficient pancreas, $n = 3$). Values are means ± SEM.

conducted with mouse strains expressing Cre recombinase in the pancreatic progenitors. This prevented to draw conclusions about the cell type whose defects cause the pancreatic anomalies. In this paper, we show that duct-specific deletion of Hnf6 or Lkb1, two genes with functions previously linked to the cilia, leads to ciliary defects, lipomatosis, and pancreatitis. Considering the phenotypic similarities between mouse models deficient in Hnf6, Lkb1, Kif3a, and Ift88 (9–11) our data strongly suggest that ciliary defects contribute to pancreatitis and lipomatosis.

Hnf6 is required for duct morphogenesis in the developing pancreas. Constitutive deletion of Hnf6 leads to cystic ducts and defects in assembly of primary cilia (15). Interestingly, no sign of ADM and pancreatitis is observed in the Hnf6 KO mice (12). Unlike in Sox9CreER/Hnf6$^{f/-}$ mice, Hnf6 cannot be induced in acini of constitutive Hnf6 KO mice. Since induction of Hnf6 in acini is necessary for ADM, constitutive Hnf6 KO mice cannot develop ADM (27). In contrast ductal deletion of Hnf6 is associated with acinar expression of this factor, thereby allowing ADM.

Lkb1 is found in primary cilia (32) and its loss in cultured fibroblasts results in disassembly of the cilium (18). In the pancreas, Lkb1 deletion at the embryonic stages leads to pancreatitis and cystic neoplasms (16). This observation is consistent with a strongly increased risk of pancreatic cancer in Peutz-Jeghers patients (PJ; OMIM entry #175200) who carry germline inactivating mutations of LKB1 (33). The present work is to our knowledge the first showing ciliary defects resulting from Lkb1 inactivation in an animal model. We suggest that pancreatic cancer risk in PJ patients and ciliary defects are linked. Whether ciliary defects directly promote cancerogenesis, or whether the cancer indirectly results from chronic pancreatitis remains to be determined. Interestingly, three genes with ciliary functions, ExoC4, Ift80, and Dock1, were identified as potentially involved in familial pancreatic cancer (34,35).

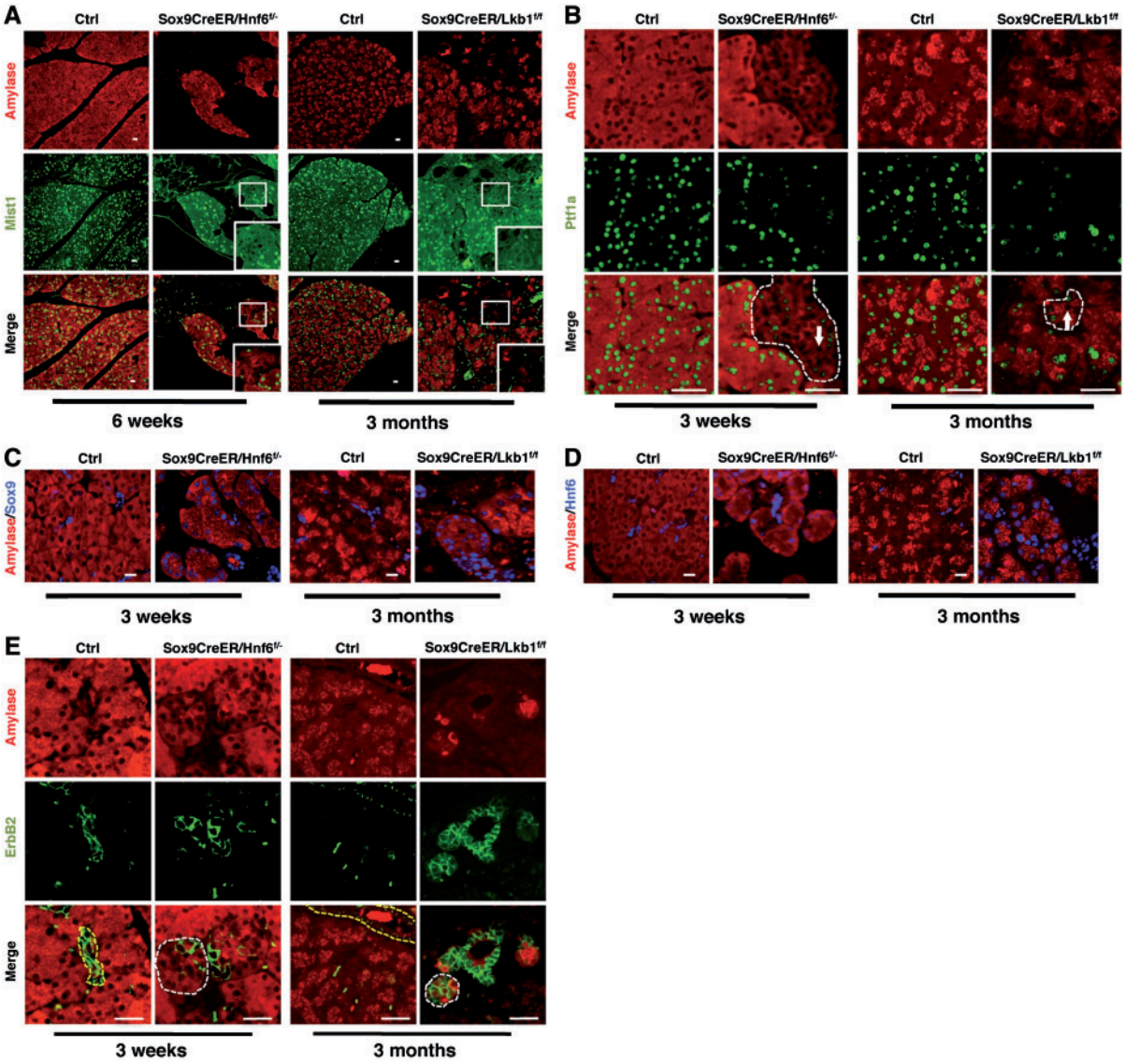

Figure 4. Ductal deletion of Hnf6 or Lkb1 leads to acinar-to-ductal metaplasia. (**A,B**) Immunofluorescence detection of the acinar markers Mist1, Ptf1a, and amylase. Dashed lines surround metaplastic acini of mutant mice in which examples of acinar nuclei that lost Ptf1a expression are shown by arrows. (**C**) Immunofluorescence labelling of the ductal transcription factor Sox9 reveals extensive staining in acinar cells of Sox9CreER/Hnf6$^{f/-}$ or Lkb1$^{f/f}$ mice compared to control mice in which Sox9 expression is restricted to ductal cells. (**D**) Expression of Hnf6 is high in ducts and absent in acinar cells in control pancreas. In Sox9CreER/Hnf6$^{f/-}$ or Lkb1$^{f/f}$ pancreas, expression of Hnf6 is increased in metaplastic acinar cells. (**E**) The EGFR signalling pathway member ErbB2 is ectopically induced in acinar cells of Sox9CreER/Hnf6$^{f/-}$ pancreata compared to control tissue. Yellow dashed lines surround ducts of control mice labelled by ErbB2. White dashed lines surround metaplastic acini of mutant mice in which ErbB2 expression is seen. Scale bar= 50 μm (panels A, C and D) and 20 μm (panels B and E).

Moreover, ADPKD patients sometimes develop intraductal papillary mucinous tumour (36), a neoplasm arising from pancreatic ductal cells.

Duct dilations in our mouse models may result from duct obstruction and such obstruction may cause pancreatitis. We do not favour this hypothesis. First, duct obstruction is expected to generate an acute response, while our phenotypes develop slowly and gradually increase over several weeks. Second, duct obstruction in mice, as seen after pancreatic duct ligation, generates a massive inflammatory response with little or no lipomatosis (27). Instead, discrete inflammatory infiltrates and very significant lipomatosis are monitored in the absence of ductal expression of Lkb1 or Hnf6.

More extensive duct dilatation is seen in the Hnf6-deficient duct cells, compared to the Lkb1-deficient cells. In contrast, ductal cell proliferation is significantly increased in Sox9CreER/Lkb1$^{f/-}$ mice whereas no significant increase is observed in Sox9CreER/Hnf6$^{f/-}$ mice. This could indicate that the increased ductal proliferation is not the driving force of the duct dilations seen in our models. The issue of increased cell proliferation in duct dilation is debated in the literature and in this context, a role for the planar cell polarity pathway has been suggested (37). Thus, this pathway could be more perturbed in Sox9CreER/Hnf6$^{f/-}$ mice, explaining that duct dilation is more important in this model, in comparison to the Lkb1-deficient model. More experiments will be required to clarify this point.

Unlike in Kif3a-deficient pancreata (11), Hnf6- and Lkb1-deficient duct cells are not devoid of cilia but show short cilia with a swollen tip: ciliary proteins, like acetylated tubulin and

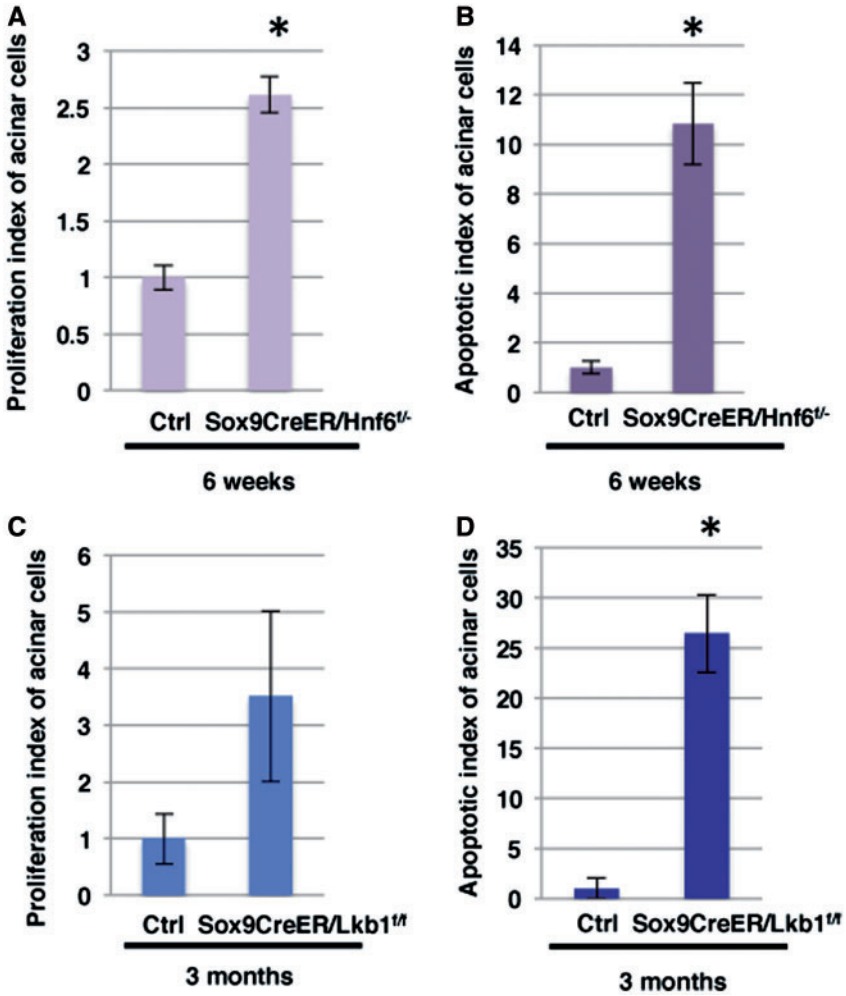

Figure 5. Acinar proliferation and apoptosis are increased in mutant pancreata. (**A**) Proliferation indexes of acinar cells are given as the percentage of Ptf1a-positive cells expressing Ki67 (6-week old animals, control, $n = 5$, Hnf6 mutant, $n = 3$). At 6 weeks, proliferation is significantly increased by 2.5-fold (2.7 ± 0.3 vs 7.0 ± 0.4, $^*P < 0.05$). (**B**) Quantification of apoptotic cells is measured as the number of cells positive for TUNEL staining per pancreas field (control, $n = 3$, Hnf6 mutant, $n = 3$). TUNEL staining shows increased apoptosis in mutant mice at 6 weeks by 10.8-fold (0.1 ± 0.03 vs 1.4 ± 0.2, $^*P < 0.05$). (**C**) Sox9CreER/Lkb1$^{f/f}$ mice show an increased though not statistically significant proliferation of acinar cells (control, $n = 3$, Lkb1, $n = 3$). (**D**) TUNEL staining shows increased apoptosis in mutant mice at 3 months by 26.4-fold (0.02 ± 0.02 vs 0.6 ± 0.08, $^*P < 0.05$. Control, $n = 3$, Lkb1 mutant, $n = 3$). Values are means ± sem.

Arl13b, accumulated at the ciliary tips. Similar ciliary morphology is found when expression of retrograde IFT proteins, such as Dync2h1, Rp2, Ift122, and a subset of Bardet-Biedl syndrome proteins (38–40), is affected. This suggests that in the absence of Hnf6 or Lkb1, retrograde IFT is defective with accumulation of proteins at the apex of the cilium.

In conclusion, our results support a model in which perturbed ductal homeostasis resulting from ciliary defects leads to lipomatosis and acinar injuries. Therefore, we suggest that a ciliopathy may be a cause of idiopathic pancreatitis and eventually contribute to cancerogenesis.

Materials and Methods

Mice

All animal experiments were performed with the approval of the animal welfare committee of the University of Louvain Medical School. Mice received humane care according to the criteria listed by the National Academy of Sciences. All strains were maintained in an enriched CD1 background.

Hnf6$^{+/-}$, Hnf6$^{f/f}$, Lkb1$^{f/f}$, Sox9-CreER, Rosa LSL YFP, Elastase-tTA, Rosa FSF YFP mice have been described (12,19–21,24–26). The Tg.TetO-FlpO mice express the codon optimized version of the Flp recombinase (41) under the control of the tetO-operator and minimal CMV promoter (to be published in details elsewhere). Control mice refer to Sox9CreER/Hnf6$^{f/+}$, Hnf6$^{+/-}$, Hnf6$^{f/-}$, Sox9CreER/Lkb1$^{f/+}$, or Lkb1$^{f/+}$ mice, as no pancreatic phenotype was observed in these different genotypes.

Tamoxifen treatment

Nursing mothers were treated with an intraperitoneal injection of 100 μL tamoxifen (Sigma-Aldrich, Saint-Louis, Missouri, USA) dissolved in corn oil (Sigma) at a concentration of 30 mg/ml combined with the gavage of another 100 μL on days 2, 6 and 10 after birth.

Immunohistochemistry and immunofluorescence

Pancreata were fixed for 6 hours in 4% paraformaldehyde at 4 °C prior to paraffin embedding. Serial sections (7 μm) were

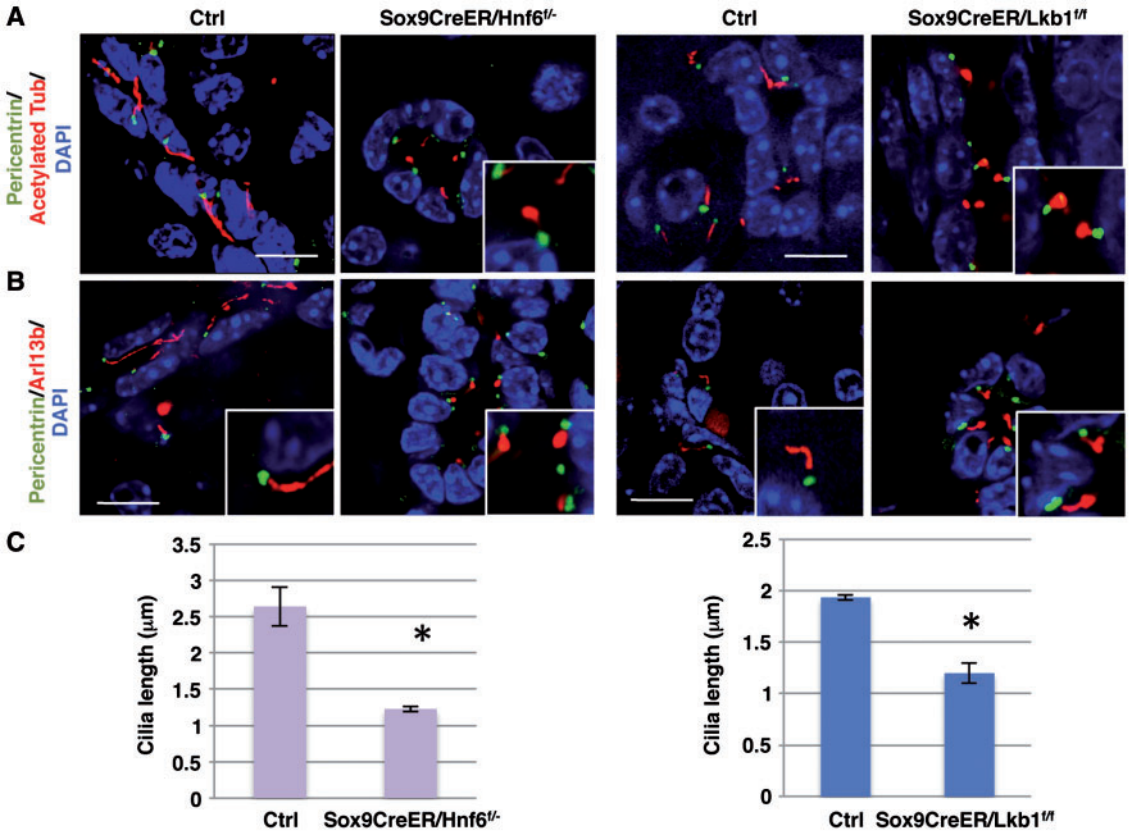

Figure 6. Primary cilia are shorter and show a swollen tip in mutant ductal cells. (**A**) Cilium axoneme was visualized using an antibody against acetylated tubulin. Centrioles located at the basal bodies were labelled by pericentrin. DAPI labels the ductal cell nuclei. Insets reveal the swelling of the ciliary tip in Hnf6- and Lkb1-deficient cells. (**B**) Labelling by Arl13b confirms cilium swelling in the mutant cells (insets). Scale bar= 10 μm. (**C**) Cilium length is reduced in both mutant pancreata. Hnf6 mutant cells show a decrease in the cilium length by 2.5-fold (2.6 ± 0.3 vs 1.2 ± 0.04, control, $n = 3$, Hnf6, $n = 3$) whereas a 1.6-fold decrease (1.9 ± 0.02 vs 1.2± 0.1, control, $n = 3$; Hnf6, $n = 3$) is observed in Lkb1 mutant cells. *$P < 0{,}05$. Values are means ± sem.

analysed. Immunofluorescence protocol was performed as in Prévot *et al.* (42). Primary antibodies are listed in Supplementary Material, Table S1. The anti-amylase antibody batch used to analyse sections from Sox9CreER/Hnf6$^{f/-}$ mice differs from the one used for analysis of Sox9Cre/Lkb1$^{f/f}$ sections, resulting in slightly different staining results. Masson's trichrome staining was achieved by deparaffinising and rehydrating the tissue, then placing the sections in Hematoxylin solution for 1 min. Slides were rinsed and placed into fuchsine-xylidine-ponceau stain for 5 min. After additional rinsing, slides were placed into 1% phosphomolybdic acid solution for 5 min and then transferred into 1% light green solution for 3 min. Slides were then rinsed with acidified water and dehydrated through a series of anhydrous alcohol before mounting. Fluorescence labelling was visualized and photographed with a Cell Observer Spinning Disk confocal microscope (Zeiss, Zaventem, Belgium). A Mirax imaging system (Zeiss) was used after histological staining.

Rabbit anti-Sox9 antibodies were raised against a peptide located between amino acids 470 and 520 of the human Sox9 protein. No cross-reactivity with Sox10 was found.

Pictures from immunolabeling or immunostaining experiments shown in the figures reflected a phenotype that was found in all mice of the genotype considered ($n \geq 3$ for each picture).

Hyperplastic area quantification

Following immunolabelling for Sox9 and Amylase, 12 non-overlapping, representative tissue fields at 25X magnification were randomly chosen to measure ductal area. For transgenic mice, only hyperplasic areas were used for quantification. Only ducts composed of more than three cells were taken into account. Axiovision software was used to measure the internal area of ducts.

Quantification of acinar cell and adipocyte area

To quantify the percentage of YFP-positive acinar cells labelled in elt-TA/Flippase/RosaFSF-YFP mice, three pancreatic sections were randomly chosen in different regions of the same pancreas. In these sections, after immunolabeling with YFP and amylase antibodies, we determined using the AxioVision SE64 Rel. 4.9.1 SP1 software (Zeiss) the YFP-positive acinar cell area (A) and the total area occupied by the acinar cells identified on the basis of the background labelling (B). The percentage of YFP-positive acini corresponded to $100 \times \frac{A}{B}$.

A similar method was used to determine the percentage of acinar cell-derived adipocytes. In this case, after immunolabelling with YFP and FABP4 antibodies, we quantified the total area of the intra-pancreatic adipocytes (C), and the area occupied by

the YFP-positive intra-pancreatic adipocytes (D). The percentage of acinar cell-derived adipocytes corresponded to $100 \times \frac{(D \times B)}{(C \times A)}$.

Proliferation and apoptosis

Proliferation of duct and acinar cells was determined by immunolabeling with Ki67 and Sox9, Hnf1β or Pft1a antibodies. Positive cells were scored from 7 non-overlapping fields at 25X magnification. The percentage of Ki67 positive cells was calculated by dividing the number of cells expressing Ki67 by the total number of cells expressing Sox9 and Hnf1β or Ptf1a. For ductal proliferation, hyperplastic areas from transgenic mice were used for counting. The level of apoptosis was determined using the transferase-mediated dUTP nick end-labelling (TUNEL, Roche Diagnostics Co.) assay according to the manufacturer's protocol. Apoptosis was quantified by counting the number of labelled nuclei per mouse (5 fields for each mouse). The percentage of TUNEL-positive cells was calculated by dividing the number of acinar cells positive expressing TUNEL staining by the total number of Ptf1a-positive acinar cells. Hyperplastic and metaplastic area were used for counting. All countings were performed with Adobe Photoshop CS5.

Quantification of cilia length

Immunofluorescent images of cilia stained for acetylated tubulin were taken using a Cell Observer Spinning Disk confocal microscope at 100X magnification (Zeiss, Zaventem, Belgium). Approximately 50 cilia were measured for each mouse ($n = 3$ for each condition). Data analysis was performed with Axiovision software.

Statistical Analysis

Statistical significance was determined using the non-parametric Mann-Whitney's U-test. Differences were considered significant for $P < 0.05$. Statistical analyses were carried out with GraphPad Prism 5.0 (GraphPad Software, Inc, La Jolla, CA, USA).

Supplementary Material

Supplementary Material is available at *HMG* online.

Acknowledgements

The authors thank Adrien Grimont, Toby Hurd, and members of the LPAD laboratory for help and discussions. They thank Vitaline Degreef for expert technical assistance, and Maike Sander, Eric Sandgren, Kei Sakamoto and Maureen Gannon for providing mouse strains used in this study.

Conflict of Interest statement. None declared.

Funding

This work was supported by grants from the Fondation contre le Cancer (Belgium); the Université catholique de Louvain; the Centre du Cancer (Cliniques universitaires St-Luc); and the COST action BM1204 EU_Pancreas. CA and LC hold a Télévie fellowship. PJ is Senior Research Associate at the FRS-FNRS (Belgium).

References

1. Fliegauf, M., Benzing, T. and Omran, H. (2007) When cilia go bad: cilia defects and ciliopathies. *Nat. Rev. Mol. Cell Biol.*, **8**, 880–893.
2. Hildebrandt, F., Benzing, T. and Katsanis, N. (2011) Ciliopathies. *N. Engl. J. Med.*, **364**, 1533–1543.
3. Basten, S.G. and Giles, R.H. (2013) Functional aspects of primary cilia in signaling, cell cycle and tumorigenesis. *Cilia*, **2**, 6.
4. May-Simera, H.L. and Kelley, M.W. (2012) Cilia, Wnt signaling, and the cytoskeleton. *Cilia*, **1**, 7.
5. Berbari, N.F., O'Connor, A.K., Haycraft, C.J. and Yoder, B.K. (2009) The primary cilium as a complex signaling center. *Curr. Biol.*, **19**, R526–R535.
6. Goetz, S.C. and Anderson, K.V. (2010) The primary cilium: a signalling centre during vertebrate development. *Nat. Rev. Genet.*, **11**, 331–344.
7. Torra, R., Nicolau, C., Badenas, C., Navarro, S., Perez, L., Estivill, X. and Darnell, A. (1997) Ultrasonographic study of pancreatic cysts in autosomal dominant polycystic kidney disease. *Clin. Nephrol.*, **47**, 19–22.
8. Basar, O., Ibis, M., Ucar, E., Ertugrul, I., Yolcu, O.F., Koklu, S., Parlak, E. and Ulker, A. (2006) Recurrent pancreatitis in a patient with autosomal-dominant polycystic kidney disease. *Pancreatology*, **6**, 160–162.
9. Cano, D.A., Murcia, N.S., Pazour, G.J. and Hebrok, M. (2004) Orpk mouse model of polycystic kidney disease reveals essential role of primary cilia in pancreatic tissue organization. *Development*, **131**, 3457–3467.
10. Zhang, Q., Davenport, J.R., Croyle, M.J., Haycraft, C.J. and Yoder, B.K. (2005) Disruption of IFT results in both exocrine and endocrine abnormalities in the pancreas of Tg737(orpk) mutant mice. *Lab. Invest.*, **85**, 45–64.
11. Cano, D.A., Sekine, S. and Hebrok, M. (2006) Primary cilia deletion in pancreatic epithelial cells results in cyst formation and pancreatitis. *Gastroenterology*, **131**, 1856–1869.
12. Jacquemin, P., Durviaux, S.M., Jensen, J., Godfraind, C., Gradwohl, G., Guillemot, F., Madsen, O.D., Carmeliet, P., Dewerchin, M., Collen, D., *et al.* (2000) Transcription factor hepatocyte nuclear factor 6 regulates pancreatic endocrine cell differentiation and controls expression of the proendocrine gene ngn3. *Mol. Cell Biol.*, **20**, 4445–4454.
13. Jacquemin, P., Yoshitomi, H., Kashima, Y., Rousseau, G.G., Lemaigre, F.P. and Zaret, K.S. (2006) An endothelial-mesenchymal relay pathway regulates early phases of pancreas development. *Dev. Biol.*, **290**, 189–199.
14. Vanhorenbeeck, V., Jenny, M., Cornut, J.F., Gradwohl, G., Lemaigre, F.P., Rousseau, G.G. and Jacquemin, P. (2007) Role of the Onecut transcription factors in pancreas morphogenesis and in pancreatic and enteric endocrine differentiation. *Dev. Biol.*, **305**, 685–694.
15. Pierreux, C.E., Poll, A.V., Kemp, C.R., Clotman, F., Maestro, M.A., Cordi, S., Ferrer, J., Leyns, L., Rousseau, G.G. and Lemaigre, F.P. (2006) The transcription factor hepatocyte nuclear factor-6 controls the development of pancreatic ducts in the mouse. *Gastroenterology*, **130**, 532–541.
16. Hezel, A.F., Gurumurthy, S., Granot, Z., Swisa, A., Chu, G.C., Bailey, G., Dor, Y., Bardeesy, N. and Depinho, R.A. (2008) Pancreatic LKB1 deletion leads to acinar polarity defects and cystic neoplasms. *Mol. Cell Biol.*, **28**, 2414–2425.

17. Boehlke, C., Kotsis, F., Patel, V., Braeg, S., Voelker, H., Bredt, S., Beyer, T., Janusch, H., Hamann, C., Godel, M., *et al.* (2010) Primary cilia regulate mTORC1 activity and cell size through Lkb1. *Nat. Cell Biol.*, **12**, 1115–1122.
18. Jacob, L.S., Wu, X., Dodge, M.E., Fan, C.W., Kulak, O., Chen, B., Tang, W., Wang, B., Amatruda, J.F. and Lum, L. (2011) Genome-wide RNAi screen reveals disease-associated genes that are common to Hedgehog and Wnt signaling. *Sci. Signal.*, **4**, ra4.
19. Zhang, H., Ables, E.T., Pope, C.F., Washington, M.K., Hipkens, S., Means, A.L., Path, G., Seufert, J., Costa, R.H., Leiter, A.B., *et al.* (2009) Multiple, temporal-specific roles for HNF6 in pancreatic endocrine and ductal differentiation. *Mech. Dev.*, **126**, 958–973.
20. Kopp, J.L., Dubois, C.L., Schaffer, A.E., Hao, E., Shih, H.P., Seymour, P.A., Ma, J. and Sander, M. (2011) Sox9+ ductal cells are multipotent progenitors throughout development but do not produce new endocrine cells in the normal or injured adult pancreas. *Development*, **138**, 653–665.
21. Sakamoto, K., McCarthy, A., Smith, D., Green, K.A., Grahame Hardie, D., Ashworth, A. and Alessi, D.R. (2005) Deficiency of LKB1 in skeletal muscle prevents AMPK activation and glucose uptake during contraction. *Embo J.*, **24**, 1810–1820.
22. Bonal, C., Thorel, F., Ait-Lounis, A., Reith, W., Trumpp, A. and Herrera, P.L. (2009) Pancreatic inactivation of c-Myc decreases acinar mass and transdifferentiates acinar cells into adipocytes in mice. *Gastroenterology*, **136**, 309–319 e309.
23. Martinelli, P., Canamero, M., del Pozo, N., Madriles, F., Zapata, A. and Real, F.X. (2013) Gata6 is required for complete acinar differentiation and maintenance of the exocrine pancreas in adult mice. *Gut*, **62**, 1481–1488.
24. Guerra, C., Schuhmacher, A.J., Canamero, M., Grippo, P.J., Verdaguer, L., Perez-Gallego, L., Dubus, P., Sandgren, E.P. and Barbacid, M. (2007) Chronic pancreatitis is essential for induction of pancreatic ductal adenocarcinoma by K-Ras oncogenes in adult mice. *Cancer Cell*, **11**, 291–302.
25. Sousa, V.H., Miyoshi, G., Hjerling-Leffler, J., Karayannis, T. and Fishell, G. (2009) Characterization of Nkx6-2-derived neocortical interneuron lineages. *Cereb. Cortex.*, **19 Suppl 1**, i1–10.
26. Srinivas, S., Watanabe, T., Lin, C.S., William, C.M., Tanabe, Y., Jessell, T.M. and Costantini, F. (2001) Cre reporter strains produced by targeted insertion of EYFP and ECFP into the ROSA26 locus. *BMC Dev. Biol.*, **1**, 4.
27. Prevot, P.P., Simion, A., Grimont, A., Colletti, M., Khalaileh, A., Van den Steen, G., Sempoux, C., Xu, X., Roelants, V., Hald, J., *et al.* (2012) Role of the ductal transcription factors HNF6 and Sox9 in pancreatic acinar-to-ductal metaplasia. *Gut*, **61**, 1723–1732.
28. Zhu, L., Shi, G., Schmidt, C.M., Hruban, R.H. and Konieczny, S.F. (2007) Acinar cells contribute to the molecular heterogeneity of pancreatic intraepithelial neoplasia. *Am. J. Pathol.*, **171**, 263–273.
29. Grimont, A., Pinho, A.V., Cowley, M.J., Augereau, C., Mawson, A., Giry-Laterriere, M., Van den Steen, G., Waddell, N., Pajic, M., Sempoux, C., *et al.* (2015) SOX9 regulates ERBB signalling in pancreatic cancer development. *Gut*, **64**, 1790–1799.
30. Larkins, C.E., Aviles, G.D., East, M.P., Kahn, R.A. and Caspary, T. (2011) Arl13b regulates ciliogenesis and the dynamic localization of Shh signaling proteins. *Mol. Biol. Cell*, **22**, 4694–4703.
31. Gerdes, J.M., Davis, E.E. and Katsanis, N. (2009) The vertebrate primary cilium in development, homeostasis, and disease. *Cell*, **137**, 32–45.
32. Mick, D.U., Rodrigues, R.B., Leib, R.D., Adams, C.M., Chien, A.S., Gygi, S.P. and Nachury, M.V. (2015) Proteomics of Primary Cilia by Proximity Labeling. *Dev. Cell*, **35**, 497–512.
33. Giardiello, F.M., Brensinger, J.D., Tersmette, A.C., Goodman, S.N., Petersen, G.M., Booker, S.V., Cruz-Correa, M. and Offerhaus, J.A. (2000) Very high risk of cancer in familial Peutz-Jeghers syndrome. *Gastroenterology*, **119**, 1447–1453.
34. Lucito, R., Suresh, S., Walter, K., Pandey, A., Lakshmi, B., Krasnitz, A., Sebat, J., Wigler, M., Klein, A.P., Brune, K., *et al.* (2007) Copy-number variants in patients with a strong family history of pancreatic cancer. *Cancer Biol. Ther.*, **6**, 1592–1599.
35. Al-Sukhni, W., Joe, S., Lionel, A.C., Zwingerman, N., Zogopoulos, G., Marshall, C.R., Borgida, A., Holter, S., Gropper, A., Moore, S., *et al.* (2012) Identification of germline genomic copy number variation in familial pancreatic cancer. *Hum. Genet.*, **131**, 1481–1494.
36. Naitoh, H., Shoji, H., Ishikawa, I., Watanabe, R., Furuta, Y., Tomozawa, S., Igarashi, H., Shinozaki, S., Katsura, H., Onozato, R., *et al.* (2005) Intraductal papillary mucinous tumor of the pancreas associated with autosomal dominant polycystic kidney disease. *J. Gastrointest. Surg.*, **9**, 843–845.
37. Fischer, E., Legue, E., Doyen, A., Nato, F., Nicolas, J.F., Torres, V., Yaniv, M. and Pontoglio, M. (2006) Defective planar cell polarity in polycystic kidney disease. *Nat. Genet.*, **38**, 21–23.
38. Ocbina, P.J., Eggenschwiler, J.T., Moskowitz, I. and Anderson, K.V. (2011) Complex interactions between genes controlling trafficking in primary cilia. *Nat. Genet.*, **43**, 547–553.
39. Hurd, T., Zhou, W., Jenkins, P., Liu, C.J., Swaroop, A., Khanna, H., Martens, J., Hildebrandt, F. and Margolis, B. (2010) The retinitis pigmentosa protein RP2 interacts with polycystin 2 and regulates cilia-mediated vertebrate development. *Hum. Mol. Genet.*, **19**, 4330–4344.
40. Qin, J., Lin, Y., Norman, R.X., Ko, H.W. and Eggenschwiler, J.T. (2011) Intraflagellar transport protein 122 antagonizes Sonic Hedgehog signaling and controls ciliary localization of pathway components. *Proc. Natl Acad. Sci. U S A*, **108**, 1456–1461.
41. Wu, Y., Wang, C., Sun, H., LeRoith, D. and Yakar, S. (2009) High-efficient FLPo deleter mice in C57BL/6J background. *PLoS One*, **4**, e8054.
42. Prevot, P.P., Augereau, C., Simion, A., Van den Steen, G., Dauguet, N., Lemaigre, F.P. and Jacquemin, P. (2013) Let-7b and miR-495 stimulate differentiation and prevent metaplasia of pancreatic acinar cells by repressing HNF6. *Gastroenterology*, **145**, 668–678 e663.